A REVIEW OF FUZZY CONTROL INTEGRATED SINGLE STAGE ZETA-SEPIC CONVERTER FOR ROBUST EV BATTERY CHARGING

¹Nikhil T. Arakhrao, ² Prof.S.H. Thakare

¹ME Student, Department of Electrical Engineering VBKCE, Malkapur, (MS) India, ²Asst. Professor, S.H. Thakare Department of Electrical Engineering VBKCE, Malkapur,(MS) India nikarakhrao@gmail.com¹

ABSTRACT

Fuzzy Controllers have been proposed for physical systems which do not lend themselves to easy and accurate mathematical modelling and crisp variables, and therefore, cannot be tackled by traditional strictly analytic control design techniques. Instead, control variables are represented by fuzzy variables which let the level of uncertainty of the variables be modelled in a systematic way A single-stage-based integrated power electronic converter has been proposed for EV Battery Charging. The proposed converter achieves all modes of vehicle operation EV Battery Charging, propulsion and regenerative braking modes with wide voltage conversion ratio (M) [M < 1 as well as M > 1] in each mode. Therefore, a wide variation of battery voltage can be charged from the universal input voltage (90–260 V) and allowing more flexible control for capturing regenerative braking energy and dclink voltage. The proposed converter has least components compared to those existing converters which have stepping up and stepping down capability in all modes. Moreover, a single switch operates in pulse width modulation in each mode of converter operation hence control system design becomes simpler and easy to implement. To correctly select the power stage switches, a loss analysis of the proposed converter has been investigated in ac/dc and dc/dc stages. Both simulation and experimental results are presented to validate the operation of the converter

INTRODUCTION

The electric vehicles are now a promising solution to curb the air pollution that uses pollution-free battery power to produce clean energy for the vehicle [1]. The EVs are combination of on-board charger, battery, and the inverter-drive system [2–5]. In majority of PEVs, a bidirectional dc/dc converter is interfaced between the battery and dc-link of machine inverter [6–8] for power flow during propulsion and regenerative braking operation. Therefore, an individual ac/dc converter is used to charge the battery from the grid side. In this conventional structure, two separate power electronic converters are needed for two independent operations (charging and discharging of the battery). The bidirectional dc/dc converter in conventional structure can be integrated with the on-board charger, to have one power electronics interface for complete operation of EVs. The overall block diagram of an integrated charger with single power electronic is shown in Fig. 1a. This integration reduces the number of components because some of the switches and inductors are utilised both in ac/dc and dc/dc stages. Therefore, reduced number of switches and inductors lead to higher power density, compact size and lower cost. In this regard, this paper proposes, a new ZETA-SEPIC-based integrated converter for EVs, as shown in Fig. 1b which has buck/boost capability in each mode of operation. In addition, buck/boost operation in each mode allows selection of wide range of the battery voltage, efficient control of dc-link voltage and capturing the regenerative braking with a wide variation of the motor speed. A comparison of existing integrated converters and other competitive converters with respect to the proposed converter is described in the following paragraph. An integrated converter in [9] utilises a number of semiconductor devices to achieve each mode; therefore, it may not be an efficiency optimised and cost-effective solution. In addition, the presence of a large number of devices, this converter requires a complex control strategy to turn on the switches. An integrated converter in [10] has only

boost charging capability; thus, the selection of wide range of battery voltages is compromised. In [11], an integrated converter does not have buck/boost operation in any mode; thus, selection of the dc-link and battery voltage range is sacrificed. A three-level quasi two-stage converter in [12] with two inductors has buck/boost operation only in charging mode as a result, aforementioned advantages of buck/boost operation in each mode is sacrificed. In [13, 14], an SEPIC-based converter has been proposed for the battery charging using three inductors and at least one extra inductor is also required for propulsion and regenerative braking modes. Thus, the increase of magnetic components has a negative effect on weight, cost and volume of the charger. Authors in [15, 16] have proposed a CuK converter based on-board battery charger, which operates only in charging mode, does not include propulsion and regenerative braking modes. A single-stage converter in [17] operates only battery charging mode using four switches, eight diodes and two inductors. However, to achieve other modes of the vehicle, some more components will be employed. Therefore, this converter will utilise a large number of active and passive components, which will have an adverse effect

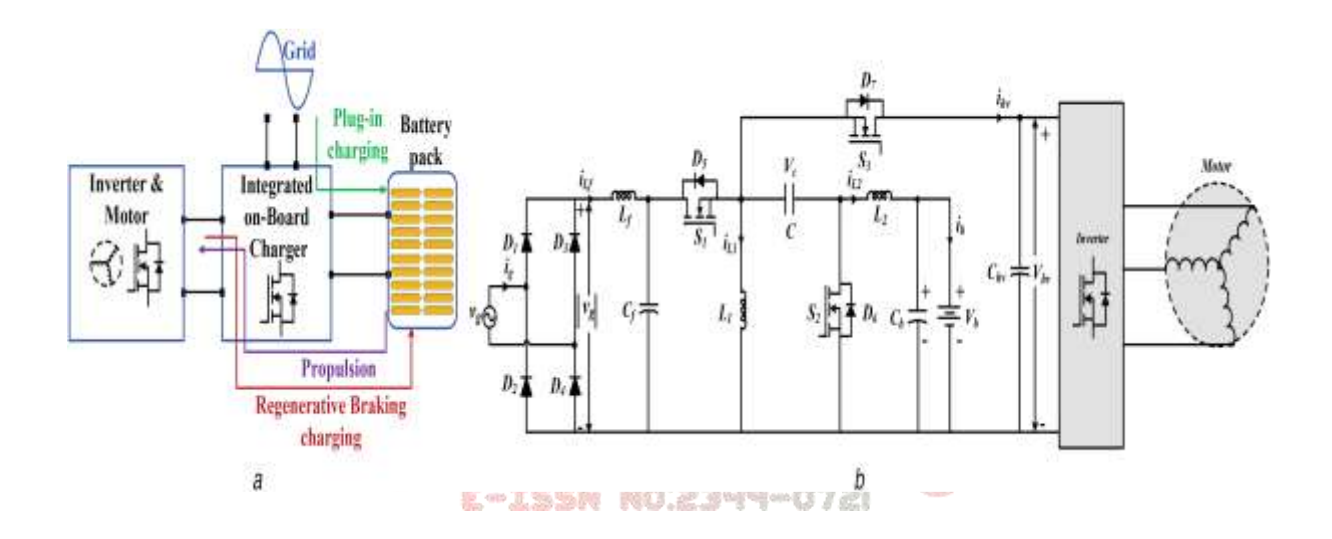


Fig. 1 Block diagram and proposed structure of the integrated converter

(a) Block diagram of PEV with on-board integrated battery charger, (b) Proposed ZETA-SEPIC-based integrated converter for PEVs

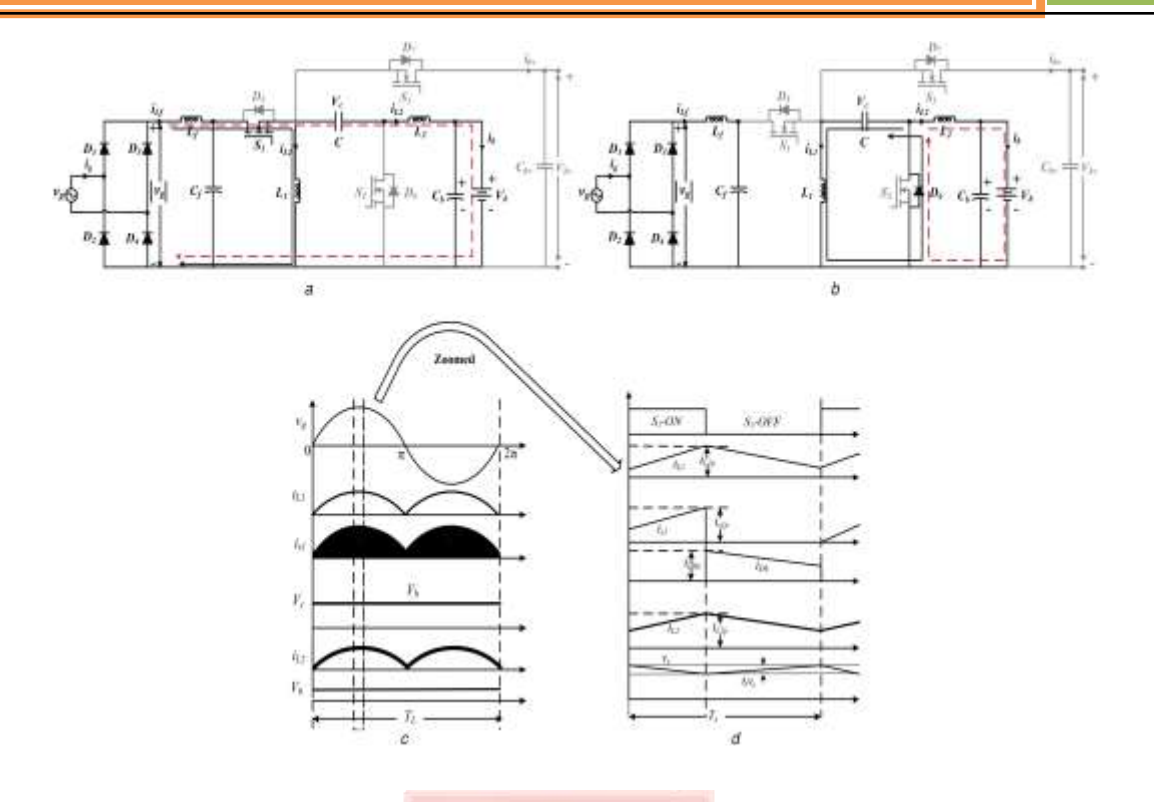


Fig. 2 Equivalent operating circuits and theoretical waveforms of plug-in charging mode

(a) Battery charging from the grid, when switch S1 is turned ON and, (b) when switch S1 is turned OFF, (c) Waveforms during one-line cycle, (d) One switching cycle

on cost and compactness of the charger. Authors in [18] have proposed front-end power factor correction (PFC) converter for EV battery charger, which is a bridgeless type converter that uses four inductors and at least one additional inductor requires to achieve other modes of the vehicle. A single-stage-based inductive charger has been proposed in [19] that provides a wide range voltage for battery charging, but this converter uses a large number of passive components and semiconductor devices; therefore, the floor area of the charger will increase and less suitable for on-board application of PEVs. Motivation of the work: The universal voltage range of single phase is around 90-260 V and a majority of commercially available battery voltage range are between 200 and 450 V [20–22]. Therefore, the buck/boost operation of converter is needed in plug-in charging mode for universal voltage supply. Moreover, in propulsion mode, usually, the battery voltage is stepped up to the dc-link voltage (inverter dc-link voltage) to propel the motor drive system. In a case of high state of charge (SOC) of the battery, the battery voltage may be more than the dc-link voltage, in such case, the dc/dc converter with buck operation is required. Furthermore, in regenerative braking, a step-down operation is typically required because the dc-link voltage usually higher or near to the battery voltage. However, at low speed, boost operation is also required to capture all the available regenerative braking energy. It is explained as: at a lower speed, the propulsion machine induces lower back electromotive force. If the generated voltage across the motor terminals is lower than the battery voltage, a bidirectional converter between the propulsion inverter and the battery must have boosting capability [10]. Therefore, the buck/boost capability of converter is also needed during regenerative braking operation. Hence, it is concluded that buck/boost operation of converter is essential in each mode of vehicle operation.

Operation of the proposed converter

The proposed integrated converter operates in three modes: battery charging from the grid (plug-in charging), propulsion, and regenerative braking of charging. In the following section, operation of converter is discussed in detailed manner

Plug-in charging mode

The plug-in charging mode of vehicle is possible only when vehicle is not in motion and then charger plug is connected to single phase supply socket to charge the battery. In this mode, the proposed converter operates as ZETA PFC converter and switch S1 is pulse width modulation (PWM) gated while switch S2 and S3 are in OFF-state. When switch S1 is turned ON, inductor L1 stores energy through the path |vg|-Lf-S1-L1-|vg| and inductor L2 stores energy through the path |vg|-Lf-S1-C-L2-Vb-|vg|, as shown in Fig. 2a. When switch S1 is turned OFF, inductor L1 discharges by supplying its stored energy to the capacitor C, and voltage across capacitor gradually increases, which is shown in Fig. 2d, and this capacitor is charged to the battery voltage Vb. While inductor L2 supplies energy to the output stage (capacitor and battery) shown in Fig. 2b and current through L2 decreases linearly, as shown in Fig. 2d. The capacitor Chv is charged to Vg, max through the body diode of S3 in very short duration then after it retains this value forever in this mode. If the duty ratio of the converter is d1 then voltage-second balance either of inductor L1 or L2 for one switching period, Ts, can be given as

$$V_{\text{gmax}} |\sin(\omega t)| * d1(t) = V_{\text{b}} * (1 - d1(t)) * T_{\text{s}}$$
 (1)

From (1), the voltage conversion ratio M1 as

$$M1 = \frac{Vb}{Vgmax|sin\omega t|} = \frac{d1(t)}{1-d1(t)}$$
 (2)

Propulsion mode

When this mode begins, battery started supplying power to the dc link of the inverter and vehicle comes in running mode. During motion of the vehicle, the SOC of the battery continuously decreases. In this mode, switches S1 and S3 are kept in OFF state using mode selector logic, and switch S2 is gated through PWM signal. When switch S2 is turned ON, inductor L2 stores energy through the path Vb-L2-S2-Vb, and capacitor C discharges through inductor L1, as shown in Fig. 3a and inductor current through L1 is

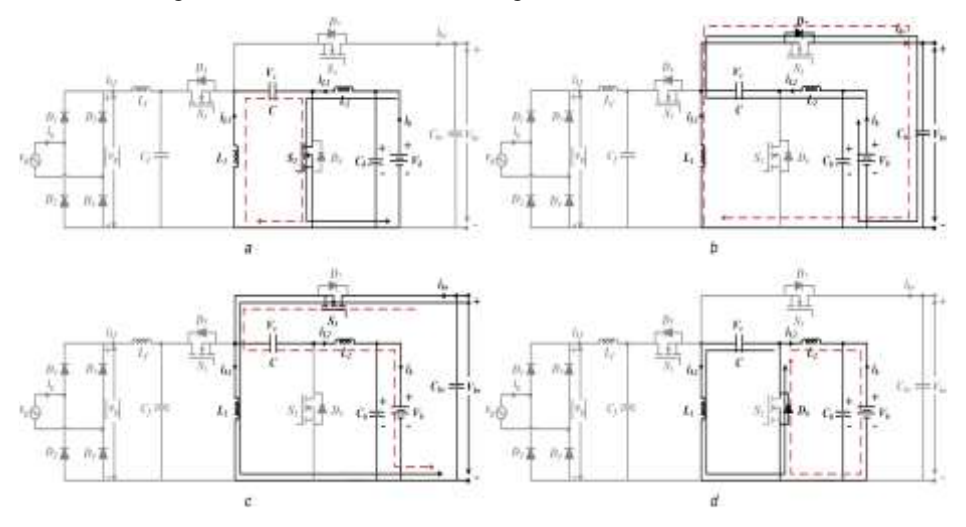


Fig. 3 Equivalent operating circuits during propulsion and regenerative braking modes

(a) Propulsion mode of operation, when switch S2 is ON, (b) When switch S2 is OFF, (c) Operation of regenerative braking, when switch S3 is ON, (d) When switch S3 is OFF

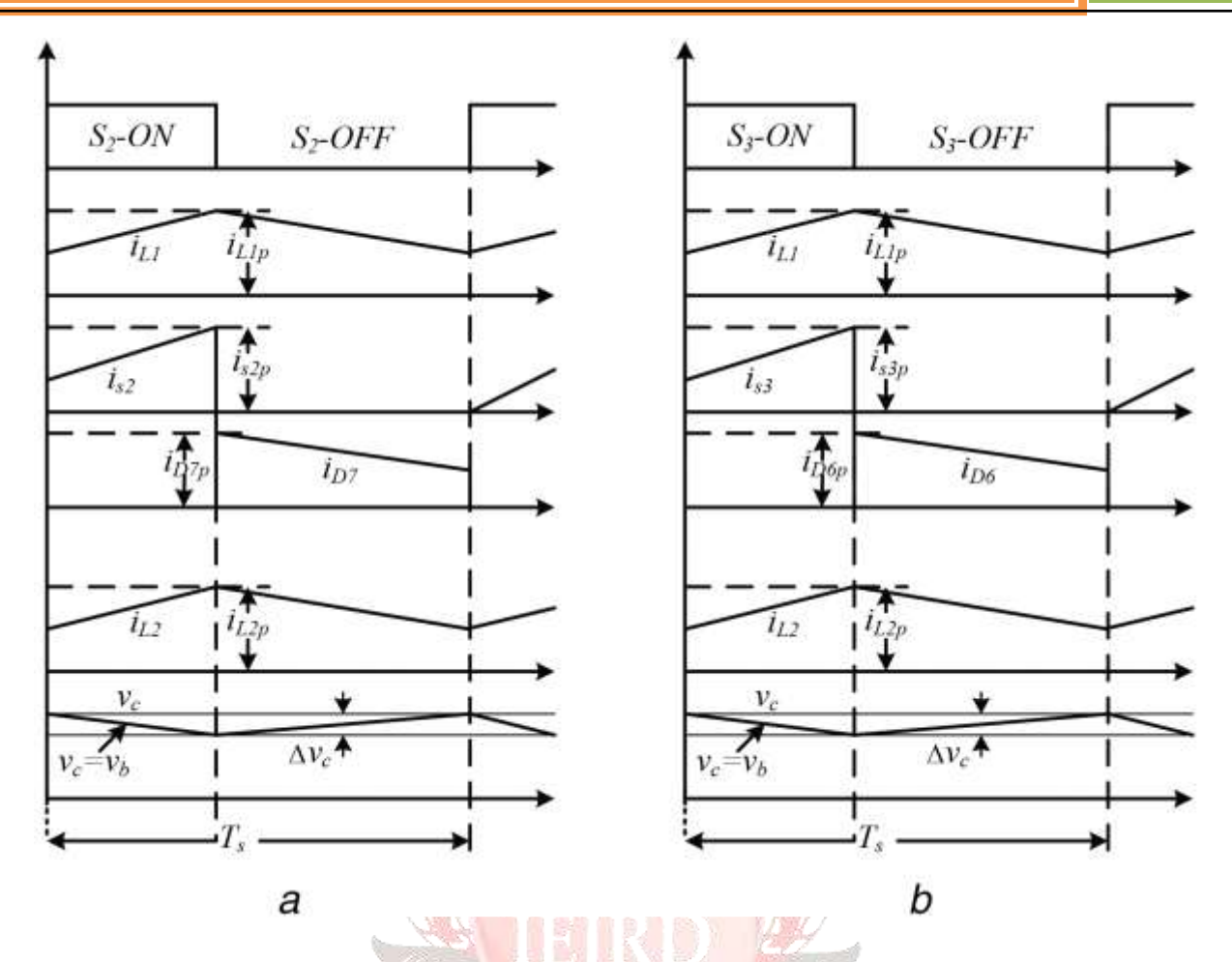


Fig. 4 Switching waveforms

(a) In propulsion mode, (b) In regenerative braking mode

OFF, inductor L2 transfers its stored energy in the capacitor C and dc-link capacitor Chv through the path Vb-L2-C-D7-Vhv-Vb and capacitor C is charged to the battery voltage. The inductor L1 transfers its stored energy to the dc-link through the path L1-D7-Vhv-L1, as shown in Fig. 3b, and current through L1 gradually decreases, which is shown in Fig. 4a. If the duty ratio of the converter is d2 and applying voltage-second balance either in inductor L1 or L2 for one switching period then one can obtain:

$$Vb * d2 * Ts = Vhv * (1 - d2) * Ts$$
 (3)

The voltage conversion ratio M2 from (3) can be expressed as

$$M2 = \frac{Vh}{Vb} = \frac{d2}{1 - d2} \tag{4}$$

Regenerative braking mode

Operation of regenerative braking mode is similar to the grid mode of operation, when switch S3 is turned ON, inductor L1 stores energy through the path Vhv S3-L1-Vhv and inductor L2 stores energy through the path Vhv-S3-C-L2-Vb-Vhv, as shown Fig. 3c. When S3 is turned OFF L1 transfers its stored energy to the capacitor (C) through the path C-L1-D6 as shown in Fig. 3d and capacitor voltage Vc gradually increases, which is shown in

Fig. 4d. While, L2 transfers its stored energy to capacitor Cb and battery (Fig. 3d). If the duty ratio of the converter is d_3 by applying voltage-second

balance either of inductor L_1 or L_2 , and one can obtain:

$$V_{hv} * d_3 * T_s = V_b * (1 - d_3) * T_s$$
 (5)

The voltage conversion ratio M3 from (5) can be expressed as

$$M3 = \frac{Vb}{Vhv} = \frac{d3}{1 - d3} \tag{6}$$

Table1

Modes	S1		S2		S3	
	Voltage	Current	Voltage	Current	Voltage	Current
plug-in charging	$ v_{g, \max} + V_{b}$	$ i_{ m g,max} +I_{ m b}$	$ v_{ m g,max} + V_{ m b}$	$ i_{ m g,max} +I_{ m b}$	$ v_{g, \text{max}} + v_{c}$	NC
propulsion	$V_{hv} + V_{b}$	NC	$V_{hv} + V_{b}$	$I_{b} + I_{hv}$	$V_{hv} + V_{b}$	I _b + I _{hv}
regenerative braking	$V_{hv} + V_b$	NC	$V_{hv} + V_{b}$	$I_{\rm b}+I_{hv}$	$V_{hv} + V_{b}$	$I_{ m b}+I_{hv}$

NC Not Conducting

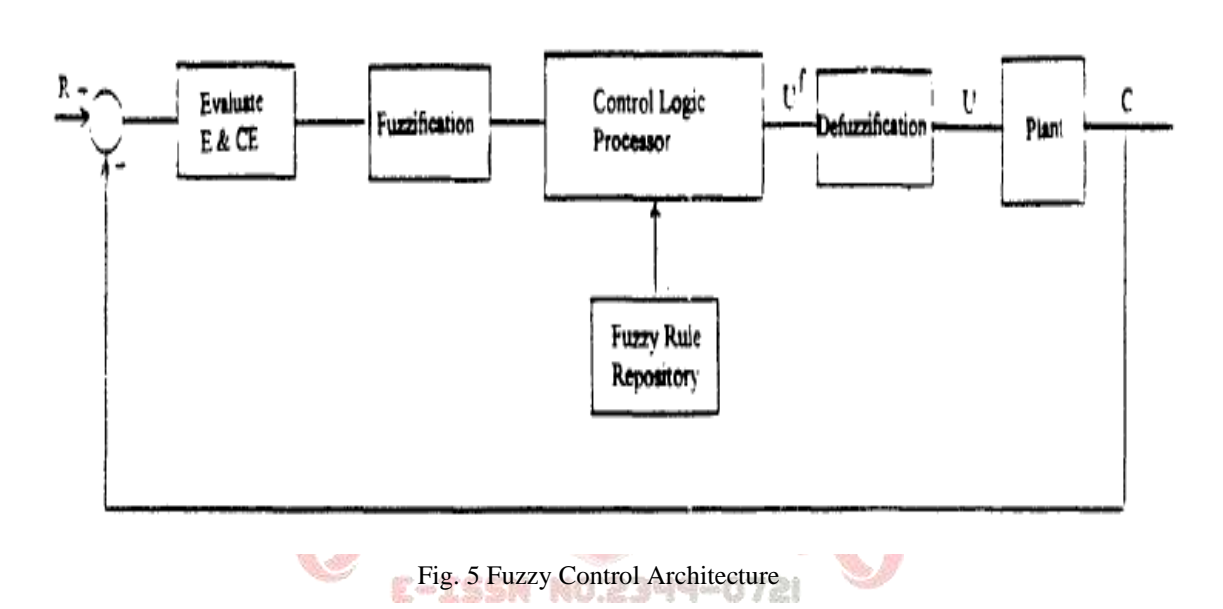
Table 2 Simulation circuit parameters

Simulation specifications: SET1	SET2			
grid voltage (Vg) 220/70.7 V	grid voltage (Vg) 220/70.7 V			
DC-link voltage (Vhv) 400/100 V	DC-link voltage (Vhv) 400/100 V			
line frequency (fL) 50/50 Hz	line frequency (fL) 50/50 Hz			
battery nominal voltage (Vb) 300/60 V	battery nominal voltage (Vb) 300/60 V			
nominal charging power (Pb) 1 kW/230 W	nominal charging power (Pb) 1 kW/230 W			
L1/L2 2/2 mH	L1/L2 2/2 mH			
switching frequency (f s) 20/20 kHz	switching frequency (f s) 20/20 kHz			
$Chv/C/Cb$ SET1 = SET2 = 550/10/2200 μ F	Chv/C/Cb SET1 = SET2 = 550/10/2200 µF			

FUZZY CONTROL THEORY

A classical control algorithm is based on mathematical model of the controlled plant (process) If an accurate model of the plant and all the values of the model parameters are available, a controller can be designed for the nominal system. However, often a physical plant is time-varying and nonlinear, and therefore hard to model .

Various corrective techniques, such as adaptive and robust algorithms are used to compensate for the lack of a well-known and deterministic plant model, as well as parameter variation. See White [13, page 93- 1401, for example Fuzzy set theory can be used to model the natural uncertainties of plant and control variables. A control algorithms which employs *fuzzy* variables in the control loop is called fuzzy control. In a *fuzzy* control algorithm, the control law is described by a set of IF . . . Then rules, similar to expert system based control. A typical rule has the following format: IF **x** is **A**nd is B THEN *z* is C where **x**, **y**, and *z* are *fuzzy* control variables, and **A**, B, and C are the *fuzzy* subsets in the universe of discourses X, Y, and Z, respectively. A typical *fuzzy* control system is shown in Figure 5. The reference input, R, and the output signal, C, are used to generate the error signal, E=R-C, and its rate of change, CE The Signal E and CE are changed to *fuzzy* variables (fuzzyfied) before being sent to the control logic processor, where the appropriate rule is retrieved from the control rule repository. According to the fired rule.



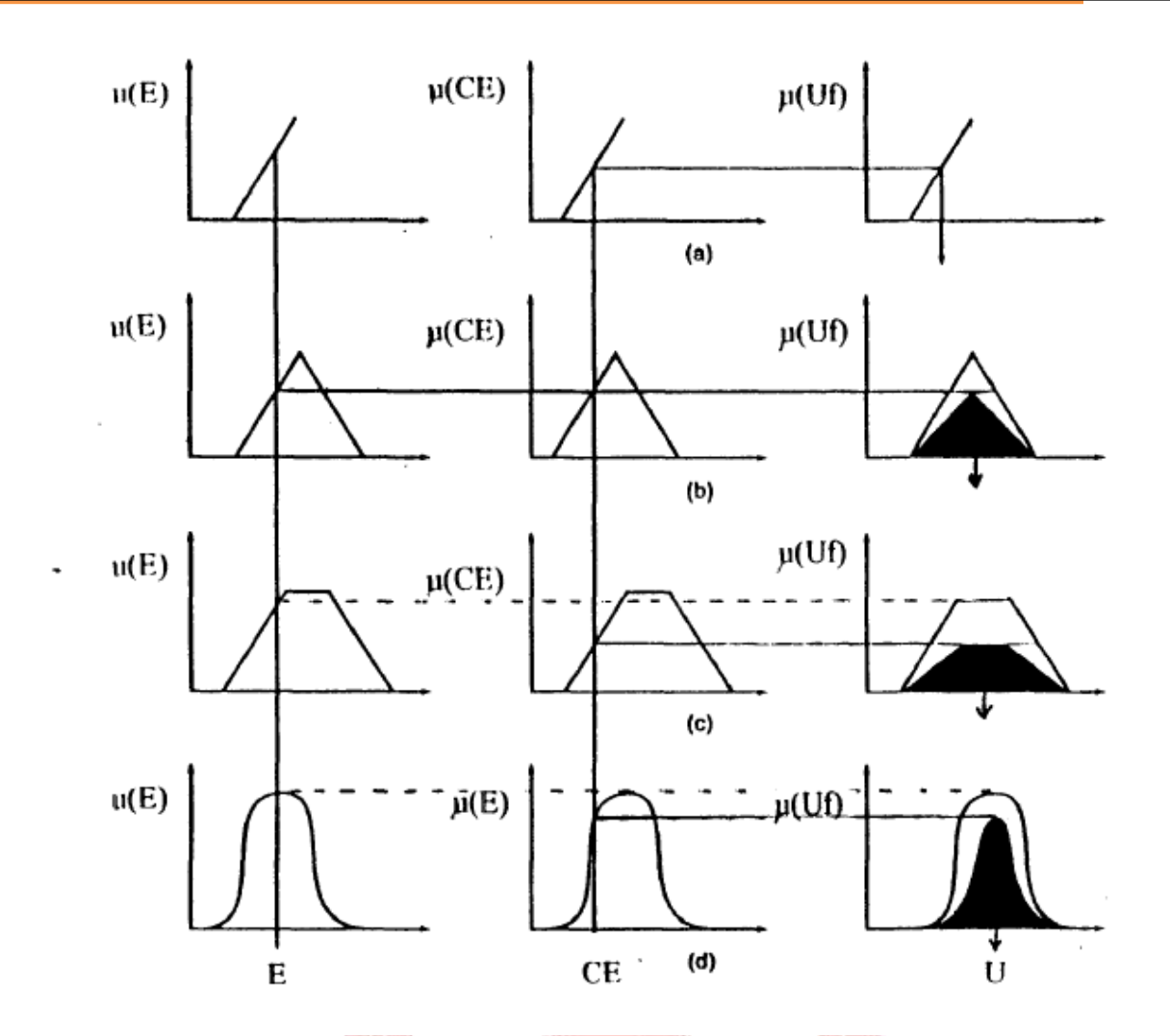


Fig 6. Examples of rule processing for different fuzzy variables

(a) Monotonic, (b) Triangular, (c) Trapezoidal., and (d) Bell shaped

CONCLUSION

In this work, a ZETA-SEPIC-based single-stage power electronics interface has been proposed for PEVs. The proposed converter operates in three modes, i.e. plug-in charging (PFC mode), propulsion and regenerative modes. In PFC and regenerative braking modes, the proposed converter operates as ZETA converter, while in propulsion mode, it operates as SEPIC converter. It means the proposed converter has buck/boost operation in each mode of converter operation without voltage reversal which allows selection of a wide range of the battery voltage, efficient control of dc-link voltage and capturing the regenerative braking energy with wide variations of the motor speed. In comparison with existing single-stage converters, the proposed converter has the least component to those converters which have buck/boost operation in each mode. The functionality and performance of the proposed integrated converter have been verified through both in simulation and hardware. The performance of control algorithm is tested with the step load variations in propulsion mode and dc-link voltage variations in regenerative braking mode. An extensive loss analysis of the proposed converter is investigated to correctly select the power stage switches. The maximum theoretical efficiency of the converter in plug-in charging, propulsion

and regenerative braking modes is found 95.9%, 97.1%, and 96.7%, respectively. While in hardware, the peak efficiency is found 94.76% at 85 W and 60 V peak grid voltage.

REFERENCES

- 1. Chan, C.C., Chau, K.T.: 'An overview of power electronics in electric vehicles', *IEEE Trans. Ind. Electron.*, 1997, **44**, (1), pp. 3–13
- 2. Emadi, A., Lee, Y.J., Rajashekara, K.: 'Power electronics and motor drives in electric, hybrid electric, and plug-in hybrid electric vehicles', IEEE Trans.Ind. Electron., 2008, 55, (6), pp. 2237–2245
- 3. Singh, A.K., Pathak, M.K.: 'An improved two-stage non-isolated converter for on-board plug-in hybrid EV battery charger'. IEEE 1st Int. Conf. Power Electronics, Intelligent Control and Energy Systems (ICPEICES), 2016. pp.1–6
- 4. Musavi, F., Edington, M., Eberle, W., et al.: 'Evaluation and efficiency comparison of front end ac-dc plug-in hybrid charger topologies', IEEE Trans. Smart Grid, 2012, 3, (1), pp. 413–421
- 5. McGrath, B.P., Holmes, D.G., McGoldrick, P.J., et al.: 'Design of a softswitched 6-kW battery charger for traction applications', IEEE Trans. Power Electron., 2007, 22, (4), pp. 1136–1144
- 6. Aharon, I., Kuperman, A.: 'Topological overview of powertrains for battery powered vehicles with range extenders', IEEE Trans. Power Electron., 2011, 26, (3), pp. 868–876
- 7. Qian, W., Cha, H., Peng, F.Z., et al.: '55-kW variable 3X DC-DC converter for plug-in hybrid electric vehicles', IEEE Trans. Power Electron., 2012, 27, (4), pp. 1668–1678
- 8. Park, T., Kim, T.: 'Novel energy conversion system based on a multimode single-leg power converter', IEEE Trans. Power Electron., 2013, 28, (1), pp.213–220
- 9. Lee, Y.J., Khaligh, A., Emadi, A.: 'Advanced integrated bidirectional AC/DC and DC/DC converter for plug-in hybrid electric vehicles', IEEE Trans. Veh. Technol., 2009, 58, (8), pp. 3970–3980
- 10. Dusmez, S., Khaligh, A.: 'A compact and integrated multifunctional power electronic interface for plug-in electric vehicles', IEEE Trans. Power Electron., 2013, 28, (12), pp. 5690–5701
- 11. Dusmez, S., Khaligh, A.: 'A charge-nonlinear-carrier-controlled reduced-part single-stage integrated power electronics interface for automotive applications', IEEE Trans. Veh. Technol., 2014, 63, (3), pp. 1091–1103
- 12. Tang, Y., Zhu, D., Jin, C., et al.: 'A three-level quasi-two-stage single-phase PFC converter with flexible output voltage and improved conversion efficiency', IEEE Trans. Power Electron., 2015, 30, (2), pp. 717–726
- 13. White D.A., et al., "Handbook of Intelligent Control," Van Nostrand Reinhold, 1992.